Wasit Journal for Pure Science

Journal Homepage: https://wjps.uowasit.edu.iq/index.php/wjps/index
e-ISSN: 2790-5241 p-ISSN: 2790-5233

New Semicarbazone-Schiff Base Coordination; Synthesis, Characterization and Biological Evaluation

Eman Ali Atiyah[1] **Enaam Ismail Yousif**[2]*

[1,2]Department of Chemistry, College of Education for Pure Science (Ibn Al-Haitham), University of Baghdad, IRAQ.

*Corresponding Author: Enaam Ismail Yousif

DOI: https://doi.org/ 10.31185/wjps.367
Received 01 March 2024; Accepted 02 May 2024; Available online 30 Jun 2024

ABSTRACT: The synthesis and characterisation of a new azo Schiff base ligand generated from a semicarbazone moiety are reported in this study, in addition to its metal complexes. The title ligand, (E)-2-((2-hydroxy-3-((E)-(2-nitrophenyl) diazenyl) naphthalen-1-yl) methylene) hydrazine-1-carboxamide (HL), was synthesised by reacting ((E)-2-hydroxy-3-((2-nitrophenyl) diazenyl)-1-naphthaldehyde) with semicarbazidein a 1:1 molar ratio. Afterward, the interplay between HL and other metal ions (Cr^{III}, Mn^{II}, Co^{II}, Ni^{II} and Cu^{II}) produced monomeric coordination complexes in a 1:1 ligand-to-metal ratio. A range of spectroscopic and analytical techniques, such as magnetic susceptibility, conductance tests, ^{1}H and ^{13}C-NMR, FT-IR, electronic and mass spectroscopy, and elemental microanalysis, were used to extensively characterize these complexes. The synthesis of coordination compounds with six-coordinate geometries was verified by the characterization data. The study also assessed the antimicrobial efficacy of the synthesised compounds against various bacterial and fungal species, revealing that After the complex formed, the ligand's antimicrobial activity was greatly increased.

Keywords: Antimicrobial; Azo-Schiff base; ligand ((E)-2-hydroxy-3-((2-nitrophenyl) diazenyl)-1-naphthaldehyde); Monomeric Complexes.

1. INTRODUCTION

Schiff bases were discovered in 1864 by German chemist and Nobel Prize winner Hugo Schiff. They are condensation products of primary amines and carbonyl compounds [1]. Schiff bases are crucial in the field of coordination chemistry, given their remarkable ability to interact with and form stable complexes with nearly all metal ions. This versatility positions them as a primary organic ligand in this field [2]. The presence of the azo moiety can substantially enhance both the biological and industrial applications of these compounds [3]. Schiff bases find extensive applications across various disciplines, including analytical and inorganic chemistry, as well as biological, medicinal and pharmacological areas [4,5]. Additionally, Schiff bases with an azo group are not only significant in biological systems but also used in the manufacturing of as catalysts [6], pigments and dyes [7], intermediates, and polymer stabilizers [8], corrosion inhibitors [9]. Furthermore, they are employed in ion-selective electrodes for ion sensing [10-12]. The current work focuses on synthesising a Schiff base that incorporates both azo compounds, aiming to explore its coordination capabilities and biological activities. The synthesis process involves two steps: firstly, preparing the azo species ((E)-2-hydroxy-3-((2 nitrophenyl) diazenyl)-1-naphthaldehyde) (L) and subsequently reacting it with semicarbazide to produce the target ligand HL. Recently, we reported the synthesis of azo and their complexes [13,15]. The reaction of this ligand with various metal ions (Cr^{III}, Mn^{II}, Co^{II}, Ni^{II} and Cu^{II}) in a 1:1 ligand-to-metal ratio, results in the creation of paramagnetic complexes that are monomeric. In this study, the synthetic compounds' antibacterial and antifungal characteristics were also investigated.

---

*Corresponding Author: anaam.i.y@ihcoedu.uobaghdad.edu.iq

2. EXPERIMENTAL

2.1.MATERIALS AND METHODS

The NMR spectra of the ligand, both proton (^1H) and carbon (^{13}C-NMR), were recorded on a Bruker 400 MHz spectrometer using DMSO-d_6 as the solvent. The frequencies for these measurements were 400 MHz for ^1H and 100 MHz for ^{13}C, with tetramethylsilane (TMS) being utilized as the internal standard. The FT-IR spectra were obtained using potassium bromide pellets and recorded with an FTIR-600 Fourier Transform Infrared Spectrometer across a spectral range of 4000 to 200 cm^{-1}. Positive-ion electrospray mass spectrometry analyses were performed on a Sciex ESI mass spectrometer. The melting points of substances were identified using a Stuart SMP40 electrothermal device. UV-visible spectra were collected in the spectral range of 1000 to 200 nm using a Shimadzu UV-160A spectrophotometer, with the solutions prepared in DMSO at a concentration of 10^{-3} mol L^{-1} and examined in a 1 cm quartz cuvette at room temperature. The conductivity of the solutions, with concentrations varying from 10^{-3} to 10^{-5} M in DMSO, was measured at 25 °C using a CyberScan CON 510 digital conductivity meter from Eutech Instruments. For elemental (C, H, N) and metal content analysis, a Heraeus Vario EL and a Shimadzu AA-7000 atomic absorption spectrometer were employed. The quantification of chloride ions in the complexes was executed via potentiometric titration with a Metrohm 686 Titro Processor and a 665 Dosim unit. Lastly, the magnetic properties were determined at 30 °C using a magnetic balance from Johnson Matthey.

2.2 SYNTHESIS

The following two procedures were used to create the azo Schiff ligand:

A- SYNTHESIS OF ((E)-2-hydroxy-3-((2 nitrophenyl) diazenyl)-1-naphthaldehyde) (L)

The preparation of L was based on a reported method [16,17] as follows;
In a charged 250 ml round-bottom flask with 1-amino-4-nitrobenzene (1.38g,10 mmol) and sodium nitrite (0.69g, 10 mmol) was added 20ml of a mixture of ethanol-water (10-10). In an icy bath, the mixture was chilled to between 0 and 5°C. Subsequently, 3ml of hydrochloric acid (36%) mixed over the course of an hour, 10 ml of water were added dropwise while stirring. This process yielded a diazonium salt solution, which was then reacted with a cooled solution containing 1.72g, 10mm of 2-hydroxy-1-naphthaldehyde and NaOH (0.4g, 10 mmol) in 20ml of ethanol EtOH. For two hours, the reaction mixture was left to agitate. Following the reaction, after being filtered at pH=4, the precipitate was repeatedly washedwith cold water. It was then left to dry until the pH was adjusted to 6-7. The remaining orange-red precipitate was filtered out, cleaned with 5ml of cold ethanol, and allowed to air dry. Yield: 2.40g (74.76%), with a melting point of 105-107°C.

B- SYNTHESIS OF (E)-2-((2-hydroxy-3-((E)-(2-nitrophenyl)diazenyl)naphthalen-1-yl)methylene) hydrazine-1-carboxamide (HL)

The synthesis of HL was conducted following a standard procedure outlined in reference [18]. Initially, a mixture containing semicarbazide hydrochloride (0.173g, 1.56mmol) in 10ml of hot methanol, with the addition of three drops of glacial acetic acid, was combined with (L) (0.5g, 1.56mmol), which was previously dissolved in a 20ml solution of ethanol-benzene mixture at a 1:1 ratio. The reaction mixture was heated to a temperature of 70-80°C and maintained for 6 hours. After the heating period, the solution was filtered while still hot. Subsequently, the mixture was allowed to cool and undergo slow evaporation at room temperature. The resulting orange precipitate, which formed upon cooling, was collected, separated from the solution, and then recrystallized from ethanol. The final product was air-dried. The yield of HL was 0.52 g (88%), with a melting point of 197-199ºC. ^1H NMR ^1H NMR (400 MHz, DMSO-$_6$, ppm) δ 10.344 (1H, s, O-*H*), 9.894 (1H, s, *N.H*), 8.879 (1H, s, -$N=C_2$-*H*), 8.474 (1H, s, C_9-*H*),8.393-8.374(2H,d,$C_{13,}$-*H*, *J*=7.5Hz), 8.274 (1H, s, C_{16}\`-*H*), 7.910 (1H, m, $C_{5,5}$-*H*), 7.846 (1H, m, C_{14}-*H*),7.688 (1H, m, C_{15} -*H*), 7.547-7.364(1H, d, C_6-*H*),7.215-7.193(1H, d, C_7-*H*),6.670 *(NH_2)*. The ^{13}C-NMR (100 MHz, DMSO-d_6, ppm).The spectrum indicated resonances at δ =156.33, 144.36, 140.34, 139.06, 136.87, 135.81, 133.04, 132.66 and131.80ppm are allocated to (C_{18}), (C_{12}), (C_2), (C_{13}), (C_{11}),(C_{15}) (C_4),(C_{10}) and (C_{16}), respectively. Resonances recorded at 130.38, 129.99-129.16, 128.57-128.43, 125.43, 124.88, 123.73-123.23, 118.96-118.20 and 110.29ppm were assigned (C_9), (C_8),(C_6), (C_7), (C_{14}), (C_{17}), (C_5) and (C_3) ,respectively. Peak at δ_c = 156.63ppm were related to(C=O). The spectrum revealed peak at 40.62-39.36ppm which is associated with the solvent (DMSO-d_6).

2.3 SYNTHESIS OF COMPLXEXS

Complexes were synthesised using a method similar to that implemented for the synthesis of the Cr^{III} complex. The procedure is as follows:

In a 100ml round-bottomed flask, (0.4g, 1.05mmol) of HL was dissolved in 10ml of ethanol. To this solution, a 10ml ethanolic solution of KOH (0.06g, 1.05mmol) was added. The mixture was stirred, followed by the dropwise addition of a solution of $CrCl_3.6H_2O$ (0.2g, 1.05mmol) in 5ml ethanol. The reaction mixture was then heated under reflux for 2 h. After heating, after filtering out the solid, the residue was cleaned with cold ethanol and allowed to air dry. The yield of the Cr^{III}-complex was 0.3g (58.77%) with a melting point exceeding 300°C (decomposition point). This synthesis procedure is illustrated in **Scheme 1**. For additional details such as yields, colours, amounts of metal salts utilized and the complexes' melting points, refer to **Table 1.**

Table 1. Yields, colours, metal salts quantities and melting points of HL complexes.

Complexes	Weight of metal salt(g)	Weight of complex(g)	Colour	M.p.ºC	Yield (%)
[Cr(L) H_2O] Cl.	0. 2	0.3	Green	>300*	58.77
[Mn(L) H_2O]	0.2	0.29	Reddish-brown	270-272	60.9
[Co(L) H_2O]	0.2	0.18	Dark brown	>300*	37.50
[Ni(L) H_2O]	0.2	0.19	brown	>300*	40.02
[Cu(L) H_2O]	0.18	0.3	Yellow	>300*	66.9

*= Decomposed.

2.4 MICROBIOLOGICALTION

The antimicrobial efficacy of the synthesised compounds was performed using the Kirby-Bauer disc diffusion technique. The suspended microbial colonies were brought to a turbidity level equivalent to the 0.5 McFarland criterion using an 85% sodium chloride solution. In a Petri dish, the Mueller Hinton agar surface was equally covered with this suspension. On the agar, wells were made with consistent concentration and spacing. 100 µL of the sample, dissolved in 1 mg/mL DMSO, was added to each well. The inhibition zones were assessed and compared with standard drugs during the incubation period of 24 hours at 37 °C [19]. DMSO-based control trial solutions confirmed no inherent antimicrobial activity against any of the tested bacterial strains or fungal species. Four bacterial strains were used to assess the synthesized (HL) and its metal complexes' antibacterial activity: *Staphylococcus aureus, Staphylococcus epidermidis (G+), Escherichia coli* and *klebsiella species(G−)* using Norfloxacin (NOR10), Cefriaxone (CR30), Cefoxitin (FOX30), AMPicillin (AM10) and Tetracycline (TE30) as a standard drugs and type from the fungi species covered *Candida albicaus.*, using Clotrimazole (CC10), Fluconazole (FLC10), A MPhotericin (AP100) and Ketoconazole (KT10)as a standard drug.

3.RESULTS AND DISCUSSION

The synthesis of the azo Schiff base ligand, (E)-2-((2-hydroxy-3-((E)-(2-nitrophenyl) diazenyl) naphthalen-1-yl) methylene) hydrazine-1-carboxamide (HL), was achieved by reacting (L) with semicarbazide hydrochloride in a 1:1 molar ratio in ethanol (**Figure 1**). This multidentate azo Schiff ligand, potentially monobasic, was reacted with metal chlorides of Cr^{III}, Mn^{II}, Co^{II}, Ni^{II} and Cu^{II} in a 1:1 ligand-to-metal (L:M) molar ratio. This yielded monomeric paramagnetic coordination compounds with six-coordinate geometries, with general formulas [Cr(L) H_2O].Cl and [M(L)H_2O] (where M=Mn^{II}, Co^{II}, Ni^{II} and Cu^{II}), as shown in **Scheme 1**. The isolated monomeric complexes are air-stable solids, soluble in DMSO and DMF. The computed values and the microanalysis results, which included the compounds' metal and chloride contents, matched rather well. (**Table 2**). In DMSO solutions, molar conductance measurements revealed that the complexes are nonelectrolytes, except for the [Cr(L) H_2O].Cl complex, which demonstrated electrolytic behaviour in a 1:1 ratio.

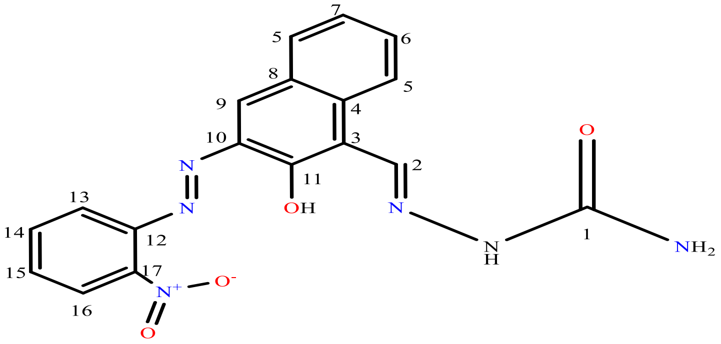

Figure 1. Chemical structure of HL.

Table 2. Microanalysis and physical characteristics of HL and its complexes.

Complex	Molecular formula	M.Wt	Micro analysis found, (calculated)%				
			C	H	N	M	Cl
[Cr(L) H2O].Cl	$C_{18}H_{15}ClCrN_6O_5$	482.80	(44.78) 44.11	(3.13) 3.01	(17.41) 17.35	(10.77) 10.26	(7.34) (7.12)
[Mn(L) H2O]	$C_{18}H_{15}MnN_6O_5$	450.29	(48.01) 47.88	(3.36) 3.21	(18.66) 18.25	(12.20) 12.00	-
[Co(L) H2O]	$C_{18}H_{15}CoN_6O_5$	453. 96	(47.58) 47.24	(3.30) 3.10	(18.50) 18.07	(12.98) 12.50	-
[Ni(L) H2O]	$C_{18}H_{15}NiN_6O_5$	453.69	(47.60) 47.31	(3.33) 3.13	(18.51) 18.06	(12.93) 12.31	-
[Cu(L) H2O]	$C_{18}H_{15}CuN_6O_5$	458.90	(47.06) 46. 86	(3.26) 3.00	(18.30) 18. 09	(13.84) 13.55	-

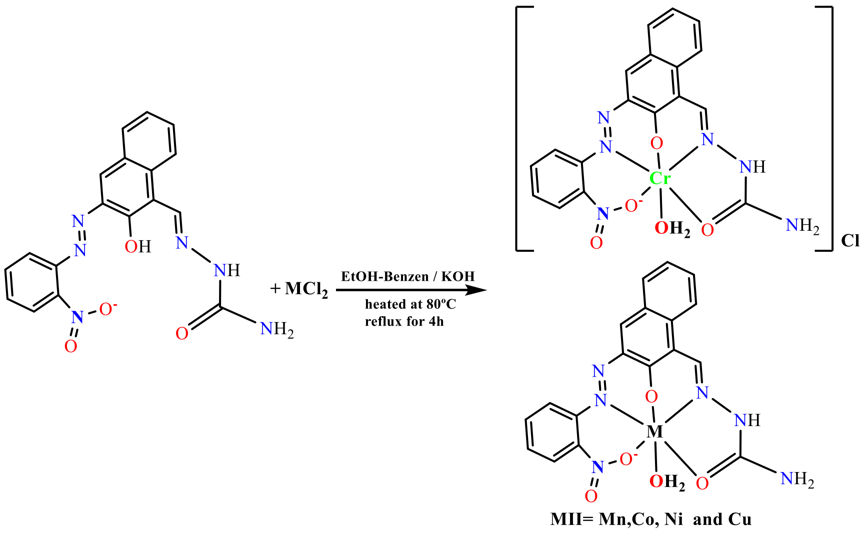

Scheme 1: HL complexes' general synthesis route.

3.1 FT-IR and NMR data

The primary infrared bands of substances **Table 3** lists them along with their tasks. A peak could be seen in the HL spectrum at 3425cm^{-1} due to the ν(OH) of the phenolic group [20]. The bands observed at 1680 and 1475 cm^{-1} are due to ν(C=O) of the carbonyl group and the ν(N=N) azo group, respectively. Upon complex formation, the carbonyl peak was shifted to a lower frequency and appeared at 1654,1647,1645,1650 and 1645cm^{-1} for the complexes indicating a strong back-bonding (dπ→ pπ*). These results validate the carbonyl moiety's participation in the coordination with the metal center [21]. In addition, The spectra of complexes showed a notable range at 1620-1616cm^{-1} that correlated to ν(C=N)imine. This band was observed in the spectrum of the ligand at 1623cm^{-1}. The bands that form upon complexation provide an explanation for the metal ion's interaction with the nitrogen atom of the azomethine group ν(C=N)imine [20]. The band that observed at 1475cm^{-1} in HL which related to ν(N=N) azo group [9]. Was shifted and appeared at 1448, 1452, 1454, 1454 and 1423cm^{-1} in 1,2,3,4 and 5, respectively. This could be related to how the nitrogen atom was implicated in the complexation. Furthermore, the spectra of the metal complexes revealed new bands around 574-507 and 497-418 cm^{-1}, which were not seen in the spectrum of the ligand, assigned to ν(M-O)$_{\text{phenolic}}$, ν(M-O) $_{\text{amide}}$ and ν(M-N), respectively [20,21]. Finally, peaks were detected at 3315, 3463, 3392, 3427 and 3313cm^{-1} in the complexes of Cr$^{(III)}$, Mn$^{(II)}$, Co$^{(II)}$, Ni$^{(II)}$ and Cu$^{(II)}$, respectively.In complex 1,2,3,4 and 5, a bands that was detected at 740, 750,744,744 and746 cm^{-1} is related to ν(Cr-O), ν(Mn-O), ν(Co-O), ν(Ni-O) and ν(Cu-O) coordinated water [9]. The peak identifications in the NMR spectra follow the numbering scheme outlined in **Figure 1**.The ^{1}H-NMR spectrum of the ligand dissolved in DMSO-d6 is illustrated in **Figure 2**. A singlet peak detected at δ_H 10.344ppm corresponds to the hydroxyl proton (O-H) of the phenol group. The location of this peak in the downfield region might indicate the presence of intramolecular hydrogen bonding with nitrogen atoms within the molecule or intermolecular hydrogen bonding with the DMSO solvent. A singlet peak detected at δ_H 9.894ppm is attributed to the hydrazinic group (N- H). Another distinct singlet peak at δ 8.879ppm corresponds to the hydrogen atom bonded to the nitrogen in the imine group (-N=C-*H*), validating the presence of an imine functional group and indicating the formation of the Schiff base. Peaks for aromatic protons are detected in the range of 8.5-7.2ppm. in the structure. The peak reported at 6.670ppm is assigned to NH_2. **Figure 3** presents the ^{13}C-NMR spectrum in DMSO-d$_6$, showing the correct count of carbon atoms in the molecule. The presence of a peak at 160.70 ppm is indicative of Schiff base formation, a conclusion further supported by the absence of a peak around 190 ppm, typically associated with the carbonyl aldehyde, confirming a condensation reaction has taken place. Additionally, the peak at 156.63ppm corresponds to the carbonyl (C=O) group within the semicarbazide component.

Table 3. **FT-IR data of the most prominent prominent bands complexes (cm^{-1}).**

Compounds	**ν(NH)$_{\text{secoam}}$**	**ν(NH$_2$)$_{\text{asy, s}}$**	**ν(C=O)$_{\text{amid}}$**	**ν(C=N)**	**ν$_{\text{ar}}$(C=C) ν N=N**	**νa N-O νs N-O**	**ν(H$_2$O) ν(M-OH$_2$)**	**ν(M-O)**	**ν(M-N)**
[Cr(L^1)H$_2$O] Cl	3407	3217 3107	1654	1618	1562 1448	1475 1392	3315 740	570 532	459 420
[Mn(L^1) H$_2$O]	3647	3433 3338	1647	1618	1598 1452	1542 1357	3463 750	574 526	497 445
[Co(L^1) H$_2$O]	3502	3315 3251	1645	1616	1548 1454	1521, 1361	3392 744	574 543	455 418
[Ni(L^1) H$_2$O]	3647	3396 3375	1650	1618	1604 1454	1542 1336	3427 744	574 507	466 426
[Cu(L^1) H$_2$O]	3436	3211 3139	1645	1620	1556 1423	1519, 1363	3313 746	572 518	455 424

3.2 MASS SPECTRUM

The HL mass spectrum was performed using an electrospray (+) mass spectroscopy, **Figure 4**. The spectrum indicated the parent ion molecule $(M)^+$ at m/z = 378.4amu (2%) calculated for $C_{18}H_{14}N_6O_4^+$ requires = 378.35 amu.

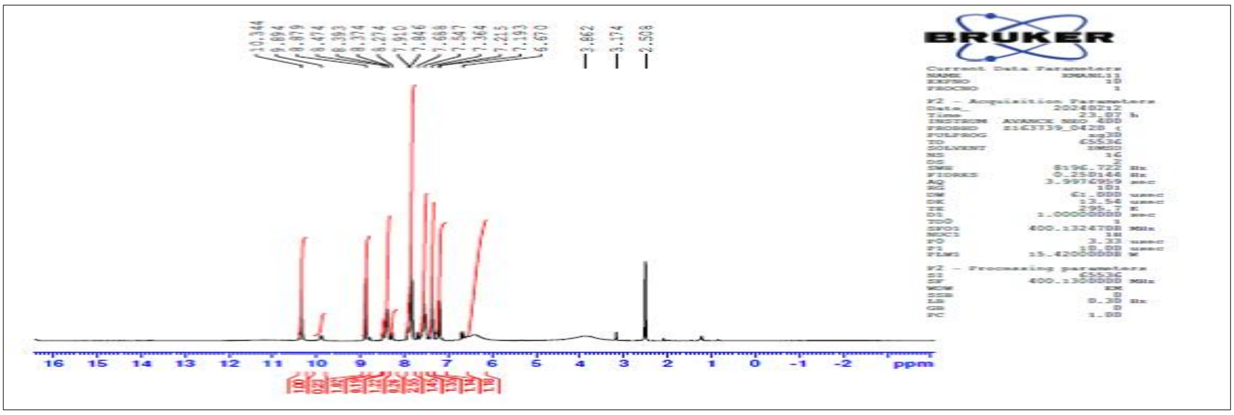

Figure 2. ^{1}**H-NMR spectrum in DMSO-**d_6 **solution of HL.**

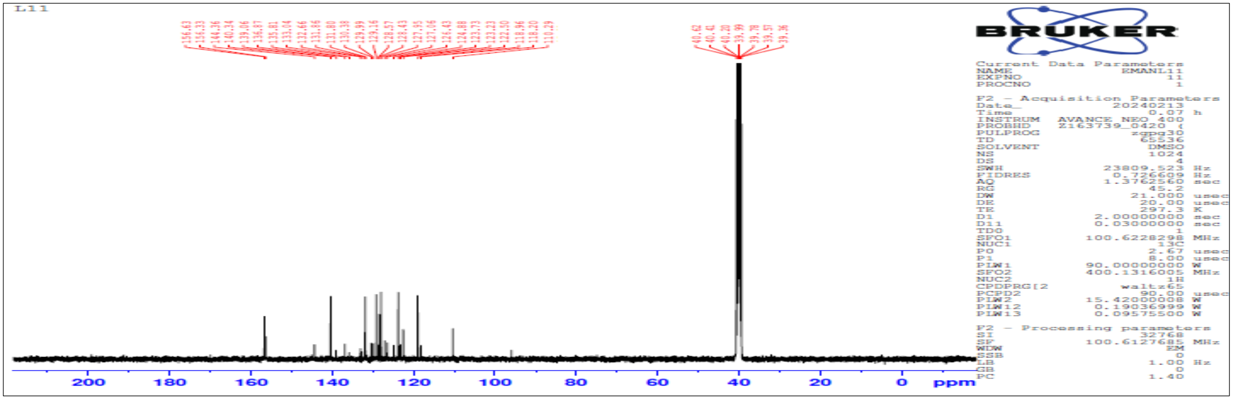

Figure 3. ^{13}**C-NMR spectrum in DMSO-**d_6 **solution of HL.**

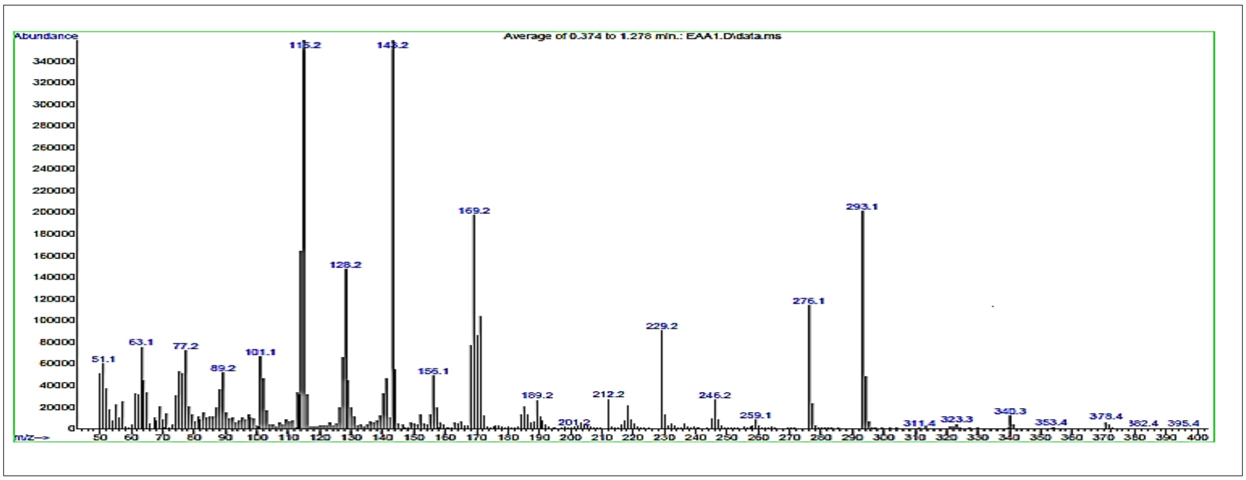

Figure 4. **The electrospray (+) mass spectrum of HL.**

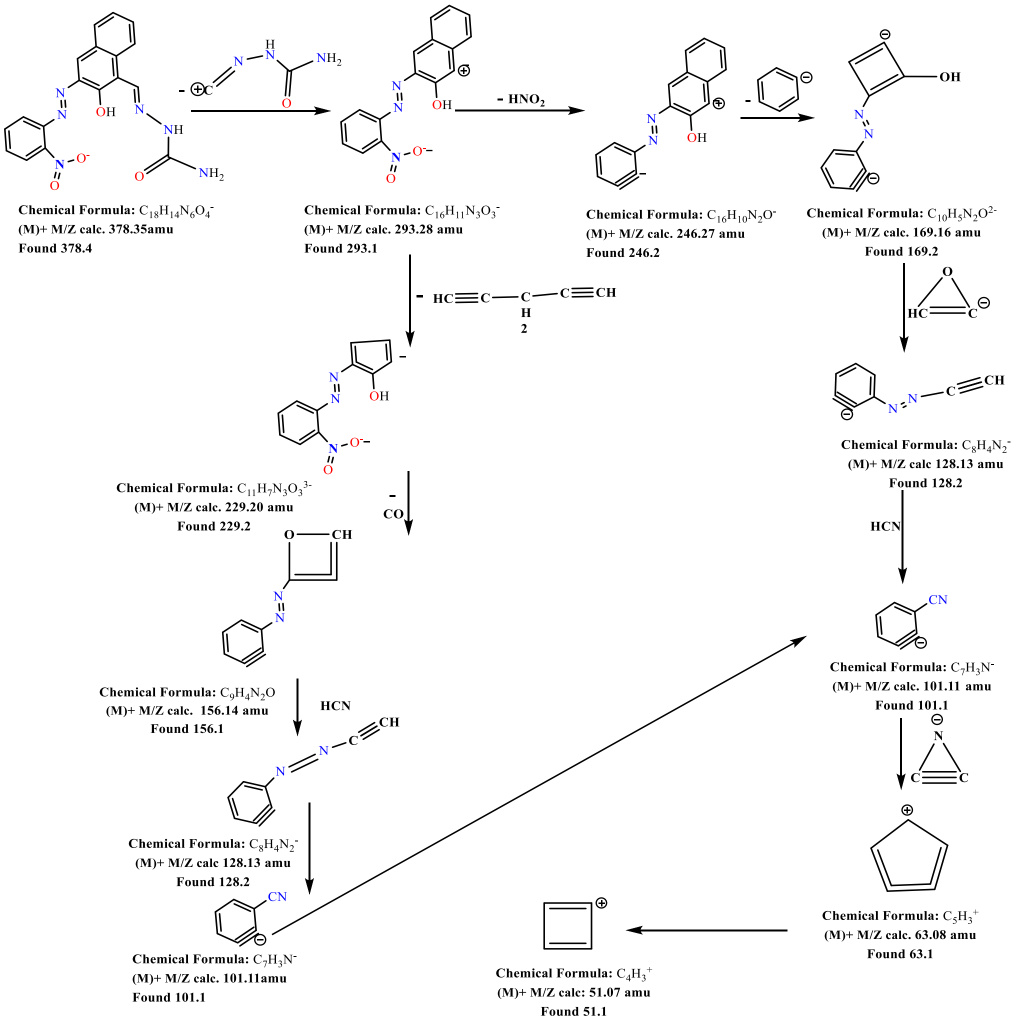

Scheme 2: **The fragmentation pattern and relative abundance of HL.**

3.3 ELECTRONIC SPECTRA AND MAGNETIC SUSCEPTIBILITY

Table 4 summarizes information on magnetic moments and electronic spectra. The electronic spectra of the complexes exhibited characteristic peaks between 251-291nm, indicative of π→π* and n→π* transitions, respectively. Additional peaks observed in the range of 311-433nm were attributed to charge transfer (C.T) phenomena [22,23]. In the Cr^{III}-complex, the electronic spectrum shows a distinctive band at 503and 682nm corresponding to the ${}^{4}A_{2}g \rightarrow {}^{2}T_{1}g$ and ${}^{4}A_{2}g \rightarrow {}^{2}T_{1}g$, revealing a distorted octahedral structure around the Cr^{III} centre. According to this view, the magnetic moment value of 3.74 BM for the Cr^{III}-complex. The [Mn(L)H$_2$O] complex displays a band at 516nm in the d-d region, ascribed to the ${}^{6}A_{1g} \rightarrow {}^{4}T_{1g}{}^{(G)}$ transition, indicative of a distorted octahedral geometry around the Mn ion. This finding is consistent with the magnetic moment measurement of 5.98 BM for the Mn^{II}-complex. For the [Co(L) H$_2$O] complex, bands in the d-d region at 667 and1015nm are observed, corresponding to the ${}^{4}T_{1g}{}^{(F)} \rightarrow {}^{4}A_{2g}{}^{(F)}$ and $4T_{1g}{}^{(F)} \rightarrow {}^{4}T_{2g}{}^{(F)}$, respectively. These bands suggest a six-coordinate complex with a distorted octahedral structure around the Co^{II} ion. The magnetic moment value µ_eff = 4.77 BM supports the octahedral configuration around the Co atom [23,24]. The Ni(II)-complex shows a peak at 486nm, assigned to the ${}^{3}A_{2}g \rightarrow {}^{3}T_{1}g^{(F)}$, indicative of a distorted octahedral geometry around the Ni atom. This geometry is corroborated by the magnetic moment measurement µ_eff = 3.1 BM for the Ni(II)-complex. Lastly, the [Cu(L)H$_2$O] complex exhibits a peak at 533 and 666nm, attributed to the ${}^{2}B_{1}g \rightarrow {}^{2}A_{2}g$ and ${}^{2}B_{1}g \rightarrow {}^{2}B_{2}g$ transition, suggesting a distorted octahedral arrangement around the Cu ion. This structural interpretation is consistent in conjunction with the magnetic moment value µ_eff = 1.89 BM for the Cu^{II} complex [23,24].

Table 4: displays the HL compounds' electronic spectra in DMSO solutions

Complex	ʎ$_{nm}$	Wave number ῡ (cm^{-1})	Molar extinction coefficient ε$_{max}$ (dm^3 mol^{-1} cm^{-1})	Assignment	μ_eff	Suggested geometry
[Cr(L) H_2O] Cl	257	38910	433	Intra-ligand $\pi \rightarrow \pi^*$,$n \rightarrow \pi^*$	3.74	Distorted octahedra
	403	24813	115	C.T		
	433	23094	117	C.T		
	503	19880	140	$^4A_2g \rightarrow {}^2T_1g$		
	682	14662	19	$^4A_2g \rightarrow {}^2T_1g$		
[Mn(L) H_2O]	251	39840	814	Intra-ligand $\pi \rightarrow \pi^*$,$n \rightarrow \pi^*$	5.98	Distorted octahedral
	311	32154	197	C.T		
	516	19379	84	$^6A_{1g} \rightarrow {}^4T_{1g}^{(G)}$		
[Co(L) H_2O]	291	34364	2408	Intra-ligand $\pi \rightarrow \pi^*$,$n \rightarrow \pi^*$	4.77	Distorted octahedral
	415	24096	920	C.T		
	432	23148	937	C.T		
	503	19880	610	C.T		
	677	14771	34	$^4T_1g^{(F)} \rightarrow {}^4A_2g^{(F)}$		
	1015	9852	21	$^4T_1g^{(F)} \rightarrow {}^4T_2g^{(F)}$		
[Ni(L) H_2O]	255	39215	1829	Intra-ligand $\pi \rightarrow \pi^*$,$n \rightarrow \pi^*$	3.1	Distorted octahedral
	370	27027	128	C.T		
	486	20576	84	$^3A_2g \rightarrow {}^3T_1g^{(F)}$		
[Cu(L) H_2O]	257	38910	410	Intra-ligand $\pi \rightarrow \pi^*$,$n \rightarrow \pi^*$	1.89	Distorted octahedral
	403	24813	121	C.T		
	433	23094	125	C.T		
	553	18083	144	$^2B_1g \rightarrow {}^2A_2g$		
	666	15015	23	$^2B_1g \rightarrow {}^2B_2g$		

4. BIOLOGICAL ACTIVITY

The antibacterial activity of the synthesized ligand (HL) and its metal complexes was evaluated using four different bacterial strains: *Staphylococcus aureus, Staphylococcus epidermidis (G+), Escherichia coli, and klebsiella species(G−),* using Norfloxacin (NOR10), Cefriaxone (CR30), Cefoxitin (FOX30), AMPicillin (AM10) and Tetracycline (TE30) as a standard drugs. Separate control experiments with DMSO confirmed it had no inherent antimicrobial effects [25]. The inhibition zone diameters were compared to the antibiotic Norfloxacin (NOR10), Cefriaxone (CR30), Cefoxitin (FOX30), AMPicillin (AM10) and Tetracycline (TE30), as shown in **Table 5, Figure 5 to 8**. Separate control experiments with DMSO confirmed it had no inherent antimicrobial effects [25]. The inhibition zone diameters were compared to the antibiotic Norfloxacin (NOR10), Cefriaxone (CR30), Cefoxitin (FOX30), AMPicillin (AM10) and Tetracycline (TE30), as shown in Table 5. The key findings were:

1. The ligand exhibits antibacterial activity against *klebsiella species.*
2. The CrIII -complex exhibits antibacterial activity against *klebsiella species* and *Staphylococcus aureus.*
. 3.The MnII and NiII complexes exhibits antibacterial activity against *Escherichia coli and klebsiella species.*
4.The CoII and CuII complexes exhibited greater potency against the tested strains.

Antifungal testing was performed against the yeast Candida albicans, using Clotrimazole (CC10), Fluconazole (FLC10), A MPhotericin (AP100) and Ketoconazole (KT10) as a standard drug. Again, DMSO controls showed no anti-fungal effects [26-30]. The obtained anti-fungal activity data against tested compounds are shown in **Table 6**, **Figure 9** The following conclusions have been pointed out;

1. All compounds displayed antifungal effects against *Candida albicaus*.
2. Complexation significantly improved antifungal activity over free HL, likely due to chelation.
3. CoII complex had the strongest inhibitory action against *Candida albicans.*
4. Clotrimazole (CC10), Fluconazole (FLC10), AMPhotericin(AP100) and Ketoconazole (KT10)greater from complexes potency against *Candida albicans.*

Table5. **Demonstrates the zones of anti-bacterial activity (mm) for HL and compounds.**

Compounds	*Escherichia coli (G−)*	*klebsiella species(G−)*	*Staphylococcus aureus (G+)*	*Staphylococcus epidermidis (G+)*
		IZ(mm)		
DMSO	-	-	-	-
Norfloxacin NOR10	30	29	30	22
Cefriaxone CR30	16	7	-	-
Cefoxitin FOX30	-	-	-	-
AMPicillin AM10	-	-	8	7
Tetracycline TE30	18	27	32	26
HL	-	10	-	-
$[Cr(L)\ H_2O]\ Cl$	-	11	9	-
$[Mn(L)(H_2O)_2]$	14	12	-	-
$[Co(L)(H_2O)_2]$	-	11	10	10
$[Ni(L)(H_2O)_2]$	13	11	-	-
$[Cu(L)(H_2O)_2]$	14	9	10	-

Table 6. **Demonstrates the zones of antifungal inhibition (mm) for HL and compounds.**

Compounds	*Candida albicaus*
DMSO	-
Clotrimazole CC10	21
Fluconazole FLC10	22
AMPhotericin AP100	12
Ketoconazole KT10	19
HL	7
$[Cr(L).\ H_2O]\ Cl$	10
$[Mn(L)\ (H_2O)_2]$	9
$[Co(L)].H_2O$	13
$[Ni(L)\ (H_2O)_2]$	9
$[Cu(L)\ (H_2O)_2]$	9

Figure 5: **The biological evaluation of HL and their complexes against Kiebsiello sp.**

Figure 6: **The biological evaluation of HL and their complexes against Escherichia cali.**

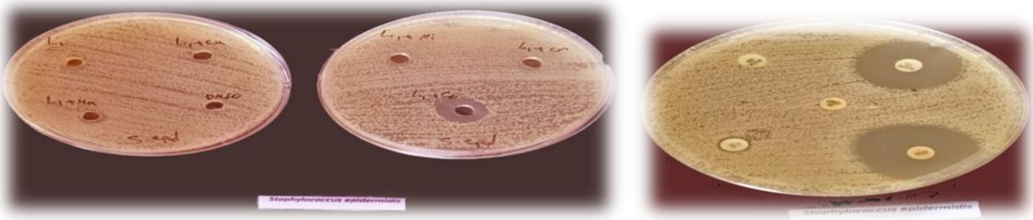

Figure 7: **The biological evaluation of HL and their complexes against Staphylococcus epidermidis.**

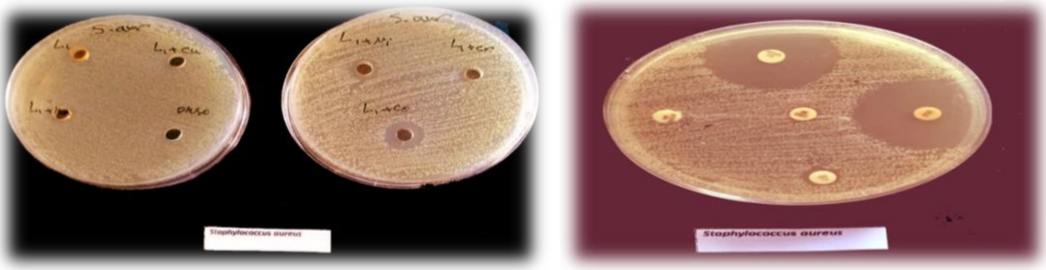

Figure 8: **The biological evaluation of HL and their complexes against Staphylococcus aureus.**

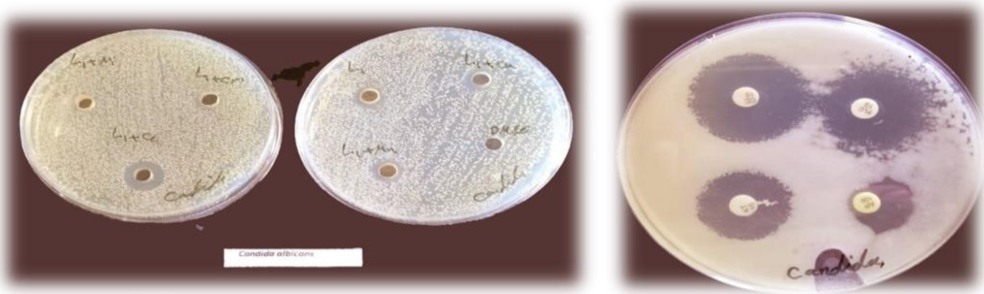

Figure 9: **The anti-fungal evaluation of HL and its complexes against *Candida albicans***

5. CONCLUSION

A new azo-Schiff base ligand (HL) and its coordination molecules with paramagnetic properties Cr^{III}, Mn^{II}, Co^{II}, Ni^{II} and Cu^{II} have been reported. The ligand (E)-2-((2-hydroxy-3-((E)-(2-nitrophenyl) diazenyl) naphthalen-1-yl) methylene) hydrazine-1-carboxamide) (HL) was synthesised *via* condensation of ((E)-2-hydroxy-3-((2 nitrophenyl) diazenyl)-1-naphthaldehyde) with semicarbazide in a 1:1 mole ratio. The reaction of HL with the metal ions at a 1:1 ligand-to-metal ratio yielded monomeric complexes, which are structurally characterised using several physicochemical techniques. The analysis suggested coordination environments of six- coordinate geometries for the metal complexes. Finally, antibacterial and antifungal testing revealed enhanced bioactivity of the metal complexes compared to the free HL ligand, highlighting the positive impacts of complexation.

REFERENCES

[1]. P. Souza, A.Jose. Garcia-Vazquez, and J.R. Masaguer, ‘‘Synthesis and characterization of copper(II) and nickel(II) complexes of the schiff base derivedfrom 2-(2-aminophenyl)benzimidazole and salicylaldehyde,’’ Transition Met. Chem.; vol.10,P.410-412, 1985.

[2].S.J.Lippard and J.M. Berg, ‘‘Principles of bioinorganic chemistry,’’ University Science Books,California,pp.411, 1994.

[3]. D.Sakthilatha, A.Deepa and R.Rajavel ‘‘Spectroscopic Characterization and In Vitro Antibacterial Activity of Some Novel Metal Complexes With Schiff Base Ligands Derived From Thiosemicarbazide,’’ Synthesis and Reactivity in Inorganic, Metal-Organic, and Nano-Metal Chemistry, 45;2, p. 286-297,2015.

[4]. K.P. Balasubramanian, R. Karvembu, R.Prabhakaran, V. Chinnusamy and K.Natarajan, ‘‘Synthesis, spectral, catalytic and antimicrobial studies of PPh3/AsPh3 complexes of Ru(II) with dibasic tridentate O, N, S donor ligands,’’ Spectrochimica Acta Part A: Molecular and Biomolecular Spectroscopy, vol.68, no.1, p. 50-54, 2007

[5]. R.Prabhakaran, R. Karvembu, T.Hashimoto, K.Shimizu, and K.Natarajan, ‘‘Formation of structurally different solvated and non-solvated [Ni(PTSC)(PPh3)](PTSC= salicylaldehyde-N-phenylthiosemicarbazide anion) crystals from single pot,’’ Inorganica chimica acta, vol.35, no.6, p.2093-2096, 2005.

[6]. S.A. Hussein, , and E. I.Yousif, ‘‘New Mannich Base (2R)-4-methyl-2-((S)(phenylamino)(p-tolyl) methyl) cyclohexan-1-one; Synthesis and Spectral Characterisation,’’ In Journal of Physics: Conference Series, Vol. 1999, No. 1, pp.012019, 2021.

[7]. A.H. Hasan, W.M. Alwan, R.M. Ahmed,and E.I.Yousif, ‘‘ Synthesis and Characterization of Some Mixed-ligand complexes Containing Azo Dye and 1,10-phenanthroline with (CoII, ZnII, CdII and HgII ions,’’IBN AL- HAITHAM J. FO R PURE & APPL SCI, vol.28, no.3, p.187-203, 2015.

[8]. H.S. Salleh , S.S Hamdan and B Yamin, ‘‘Unsaturated 15 and 16 Membered Appended Naphthalene Macrocyclic Molecules for The Development of FluorometricChemosensors. Conference Series,’’ Materials Science and Engineering, vol.172, p.1-11 2017.

[9]. A.S.A.K.A Rahman , N.J.Hussien, K.T.Abdullah , S.F.M.Yusof and E.I.Yousif, ‘‘ (Synthesis, characterization and antibacterial activity of some transition metal complexes of a new dioxime ligand). AIP Conference Proceedings,’’ vol. 2593,no.1, 060001,pp. 7, 2023.

[10]. M.N. Uddin, Z.A. Siddique, N.Mase, M.Uzzaman and W.Shumi, ‘‘Oxotitanium (IV) complexes of some bis-unsymmetric Schiff bases: Synthesis, structural elucidation and biomedical applications,’’ Applied Organometallic Chemistry,vol.33,no. 6, e4876,2019.

[11]. P.Ghosh, S. K Dey, M.H Ara, , K.Karim and A.B.M.N Islam, ‘‘A review on synthesis and versatile applications of some selected Schiff bases with their transition metal complexes,’’ Egyptian Journal of Chemistry, vol.62(Special Issue (Part 2) Innovation in Chemistry),p.523-547, 2019.

[12]. M.Abdel-Shakour, WA. El-Said, I.M Abdellah, Su, R. and A.El-Shafei, ‘‘Low-cost Schiff bases chromophores as efficient co-sensitizers for MH-13 in dye-sensitized solar cells. Journal of Materials. Vol.30, p. 5081-5091, 2019.

[13]. AH.Hasan, EI.Yousif and AK.Hussien, ‘‘Co^{II}, Ni^{II} and Cd^{II}complexes derived from mixed azo-linked Schiff-base ligands: formation, characterisation,Thermal analysis and biological study,’’ Journal of Plant Archives, Vol.20, no.1, pp. 2405-2411, 2020.

[14]. EI.Yousif,‘‘Synthesis, Characterization and Biological Study of Mixed LigandComplexes Derived from Dithiocarbamate and Azo,’’Journal of Global Pharma Technology, vol.10, no. 03, p.875-882, 2018.

[15]. EI.Yousif, ‘‘New Mixed Ligand Complexes;Synthesis, Spectral Analysis and Biological Activity,’’Journal of Global Pharma Technology, vol.11, no. 02, P.196-203, 2019.

[16]. H.Kocaokutgen, E.Erdem, ‘‘Synthesis and Spectral Characterization of Metal Complexes of 1-(2-Hydroxy-4-methylphenylazo)-2-naphthol. Synthesis and Reactivity in Inorganic and Metal-Organic Chemistry,’’vol.*34*, no. 10, pp.1843-1853, 2010.

[17]. K.Law, IW. Tarnawskyj, and PT. Lubberts, ‘‘Azo pigments and their intermediates: Effect of substitution on the diazotization and coupling reactions of o-hydroxyanilines. Dyes and pigments,’’ vol. *23*, no.4, pp.243-254, 1993.
[18]. M. Karman and G. Romanowski, ‘‘Cis-dioxidomolybdenum (VI) complexes with chiral tetradentate Schiff bases: Synthesis, spectroscopic characterization and catalytic activity in sulfoxidation and epoxidation. InorganicaChimicaActa,’’ 511, 119832, 2020.
[19]. EJ. Baron, SM.Finegold, Bailey and Scott·s,‘‘Diagnostic Microbiology, 8th Ed. Mosby,St.Louis, Company. London, P.53-62, 1990.
[20]. RM. Silverschtien, GC Bassler and TC.Morri,l “Spectrophotometers Indentification of Organic Compound*”,* Translated by Ali Hussain and Suphi Al-Azawi, 1981.

[21]. EI. Yousif, ‘‘Synthesis and Characterization of Novel Tetradentate ligand Type N4 and its Complexes With CoII,NiII,andPdII.,’’ IBN AL- HAITHAM J. FO R PURE & APPL SC I, vol. 22, no.4, p.1-13, 2017.
[22]. BK. Mohammed, E I Yousif, ‘‘(Synthesis, Structural Characterisation and Biological Activity; New Metal Complexes Derived from Semicarbazone Ligand), RevistaBionatura, Vol.8, p.2, 14 2023.
[23]. E. Ramachandran, V. Gandin, R. Bertani, P. Sgarbossa, K. Natarajan, NSP. Bhuvanesh, A. Venzo, A. Zoleoe, A. Glisenti, A. Dolmella, A. Albinati and C. Marzano, ‘‘Synthesis, characterization and cytotoxic activity of novel copper(II) complexes with aroylhydrazone derivatives of 2-Oxo-1,2- dihydrobenzo[h] quinoline-3-carbaldehyde,’’ Journal of Inorganic Biochemistry, vol.182, p.18-28, 2018.
[24]. ABP. Lever, ‘‘Inorganic Electronic Spectroscopy,’’ 2nd Ed,Esevier, New York, 1984.
[25]. RV. Singh, R Dwivedi and SC.Joshi, ‘‘Synthetic, magnetic, spectral, antimicrobial and antifertility studies of dioxomolybdenum(VI) unsymmetrical imine complexes having a $N \cap N$ donor system,’’ Transition Met. Chem., vol.29, no.1, p.70- 74, 2004.
[26]. R. Ramesh, S.Maheswaran, ‘‘Synthesis, spectra, dioxygen affinity and antifungal activity of Ru(III) Schiff base complexes,’’ J. Inorg .Biochem, vol.96, no.4, p.457-462, 2003.
[27. A. Rahman, M. Choudhary and W. Thomsen, ‘‘Bioassay Techniques for Drug Development,’’ Harwood Academic, 2001.
[28]. A H. Hasan and E I. Yousif,‘‘Formation of New Macrocyclic Complexes with bis(Dithiocarbamate) Ligand; Preparation, Structural Characterisation and Bacterial Activity,’’ IBN AL- HAITHAM J. FO R PURE & APPL. SC I, vol.29, no.3, 146-166, 2017.
[29]. EI. Yousif and AH. Hasan, ‘‘New Bis (dithiocarbamate) Ligand for Complex Formation; Synthesis, Spectral Analysis and Bacterial Activity,’’ IBN AL- HAITHAM J. FO R PURE & APPL. SC I, vol.30, no.1, p.73-87. 2017.
[30]. H M. Salh and T H Al-Noor,‘‘Preparation, Structural Characterization and Biological Activities of Curcumin-Metal(II)-L-3,4-dihydroxyphenylalanin(L-dopa)complexes,’’ Ibn Al-Haitham Journal for Pure and Applied Sciences, vol.36 ,no.1, 2023.